

See discussions, stats, and author profiles for this publication at: <https://www.researchgate.net/publication/341144999>

Enhanced Curie temperature and spin polarization in Co-based compounds under pressure: A first principles investigation

Article in *Solid State Sciences* · May 2020

DOI: 10.1016/j.solidstatesciences.2020.106257

CITATIONS

3

READS

81

4 authors:



Pachineela Rambabu

Guru Ghasidas University

25 PUBLICATIONS 141 CITATIONS

[SEE PROFILE](#)



Anuroopa Behatha

Indian Institute of Technology Hyderabad

3 PUBLICATIONS 3 CITATIONS

[SEE PROFILE](#)



M. Manivel Raja

Defence Research and Development Organisation

199 PUBLICATIONS 2,434 CITATIONS

[SEE PROFILE](#)



Kanchana Venkatakrishnan

Indian Institute of Technology Hyderabad

119 PUBLICATIONS 2,512 CITATIONS

[SEE PROFILE](#)

Some of the authors of this publication are also working on these related projects:



Magnetocaloric and Shape memory [View project](#)



GMR materials [View project](#)



Enhanced Curie temperature and spin polarization in Co-based compounds under pressure: A first principles investigation

P. Rambabu^{a,b}, B. Anuroopa^a, M. Manivel Raja^c, V. Kanchana^{a,*}

^a Department of Physics, Indian Institute of Technology Hyderabad, Kandi - 502285, Sangareddy, Telangana, India

^b Department of Pure and Applied Physics, Guru Ghasidas Vishwavidyalaya, Koni, Bilaspur, 495009, Chattisgarh, India

^c Advanced Magnetic Group, Defence Metallurgical Research Laboratory, Kancharbagh P.O- 500058, Hyderabad, Telangana, India

ARTICLE INFO

Keywords:

Electronic Topological Transitions (ETTs)

Half-metallicity

Heisenberg exchange interactions

ABSTRACT

In the present study, we report a systematic first principles study which investigates and tunes the percentage of spin polarization in few Co-based full Heusler alloys Co_2CrX ($X = \text{Al, Ga}$ and In) under hydrostatic strain. At ambient condition, Co_2CrAl exhibits half metallic nature while Co_2CrGa possesses nearly half metallic nature and Co_2CrIn shows metallic nature. Mechanical and dynamical stabilities of all the investigated compounds are confirmed using elastic tensor analysis and phonon dispersion plots respectively at ambient as well as under compression. Hydrostatic compressive strain is applied to all the systems and Co_2CrGa turned out to be a half metal at compressive strain corresponding to $V/V_0 = 0.85$ with 100% spin polarization and the percentage of spin polarization for Co_2CrIn gets enhanced as a function of compressive strain. Further, an electronic topological transition (ETT) is also observed in Co_2CrGa as a function of compressive strain corresponding to $V/V_0 = 0.85$, driving the system towards the half-metallic nature. In addition, ferromagnetic nature of all these compounds is explained by the exchange interactions at both ambient and under compression. Also, the positive pressure dependence of Curie Temperature (T_C) as a function of V/V_0 for all the compounds is studied and the highest $T_C = 646.1$ K for Co_2CrAl is observed under compression corresponding to $V/V_0 = 0.85$.

1. Introduction

Spintronics is one of the emerging areas in the technological world. This technology not only uses the charge degrees of freedom of electron but also uses its spin degrees of freedom. The practical use of spin degree of freedom covers wide range of applications such as spin-transfer torque, spin-valve device, development of magnetic storage devices etc. [1]. Several ferromagnetic materials, magnetic oxide materials, multiferroics, Heusler compounds etc. are found to have several applications [2]. Difference in the population of spin-up and spin-down states of a compound gives the percentage of spin polarization. Achieving high spin polarization at room temperature is a requirement in this field and a lot of research has been done in this field of spintronics [3–6]. There are several methods such as doping, pressure application etc. to improve the potential of a material so as to use it as spintronic material. From earlier reported experimental studies, it is found that thin films of Co_2FeSi when substituted with Boron and Gallium show a considerable increase in the Curie temperature [7,8]. Half-metallicity is also found to be preserved with this substitution. With the substitution of suitable elements to full Heusler alloys, the magnetic moment and spin polarization can be enhanced [7]. $\text{Co}_2\text{Mn}_{1-x}\text{Fe}_x\text{Sn}$ when doped

with Fe on Mn site with $x = 0.05$, the spin polarization is reported to be increased but for the substitution with $x = 0.1$ and 0.2 , the spin polarization is found to decrease [9]. The effect of pressure on Heusler compounds is also studied in the literature, and ScNiCrX ($X = \text{Al, Ga}$) [10] has been studied under pressure. The results show that half-metallicity will be retained up to certain range of pressures. Doping of certain elements to the full Heusler alloys may not change the half-metallicity, but it may enhance spin polarization up to significant value [11–14]. Disorder and doping are the mechanisms to tune the magnetic properties in magnetic materials but for spintronic applications point of view, one needs to be more worried about degree of spin polarization. Now the question is, whether these mechanisms affect the degree of spin polarization or not. From the earlier studies done on doped magnetic compounds, it was found that there is no significant effect on the half-metallicity due to disorder and doping which preserve high spin polarization in these systems [15,16].

The main application of spintronics is the fabrication of magnetic tunnel junction. The magnetic tunnel junction consists of non-magnetic layer which is sandwiched between two magnetic layers. If the spins of the both magnetic layers are aligned parallel, the resistance of the

* Corresponding author.

E-mail address: kanchana@iith.ac.in (V. Kanchana).

<https://doi.org/10.1016/j.solidstatesciences.2020.106257>

Received 6 February 2020; Received in revised form 25 April 2020; Accepted 28 April 2020

Available online 4 May 2020

1293-2558/© 2020 Elsevier Masson SAS. All rights reserved.

device will be small and if the spins of both the magnetic layers are aligned anti-parallel, the resistance of the device will be large. Therefore, the magnetization of the device can be found from the fluctuation of the resistance measured. This can act as memory sensors. The memory-storage devices developed with spin-based technology can store large amount of information and the power consumption by such devices is always low. Therefore, there has been always an interest in the study of the materials for spintronics applications. The practical application of spintronics requires materials with high spin polarization. The production of 100% spin polarization and injection of spin into devices are some of the difficulties in this field. One of the methods for obtaining large spin polarization is by applying magnetic field, but this is not feasible in the nanometer range. Conventional ferromagnets possess a spin polarization typically less than 50% and hence cannot inject electrons with large degree of spin polarization into the non-magnetic material. Half metallic compounds are very good in spin filtering applications as in these materials, only one spin state will be conducting while the other is an insulator. Heusler alloys are one of the very interesting series of compounds ever since their discovery [17]. These materials are used for spintronic applications in the form of thin films on suitable substrates. The film is expected to experience either compressive strain or tensile strain depending on the substrate selected, thermal expansion coefficient of film and substrate, process temperature etc. Hence, the study of spin polarization under hydrostatic strain on Co based Heusler alloys is aimed at enhancing the spin polarization to 100% and also to understand the effect of compressive strain on the magnetic properties of the compounds. Thus, in the present work, we intend to explore three compounds Co_2CrX ($X = \text{Al}, \text{Ga}, \text{In}$) at ambient conditions as well as under hydrostatic strain with a view of enhancing the spin polarization. The paper is organized into three subsections as Computational Methods and Theoretical Formulation, Results and discussion and Conclusion.

2. Computational methods and theoretical formulation

2.1. Computational methods

The calculations are performed using WIEN2k which is a full potential linear augmented plane wave method (FP-LAPW) [18]. The optimized lattice parameters for the three compounds Co_2CrX ($X = \text{Al}, \text{Ga}, \text{In}$) are obtained by using Birch–Murnaghan [19] equation of state in order to fit total energies as a function of primitive cell volume. The exchange correlation functional employed for the calculation is Perdew–Burke–Ernzerhof (PBE) [20] within the Generalized Gradient Approximation (GGA) method. The conventional unit cell of all these compounds has a cubic structure with interpenetrating fcc sub lattices. It has four formula units ($Z = 4$) in which, the Co is placed at $(1/4, 1/4, 1/4)$, Cr at $(0, 0, 0)$ and $X = (\text{Al}, \text{Ga})$ at $(1/2, 1/2, 1/2)$ positions in the case of Co_2CrAl and Co_2CrGa . In the case of Co_2CrIn , the position of the Co atom is at $(1/4, 1/4, 1/4)$ while the positions of Cr and In are $(1/2, 1/2, 1/2)$ and $(0, 0, 0)$ respectively. The muffin-tin sphere radii used in the calculation are 2.05 a.u for both Co and Cr, and is set to 1.93 a.u for both Al and Ga, while it is set as 2.3 a.u in the case of In, as the charge should not leak out from the sphere. The $R_{MT}^*K_{max}$ is set to 7 for all the calculations, where R_{MT} is the smallest value of muffin-tin radius and K_{max} is the maximum value of the reciprocal lattice vector. The k-point sampling was done using a mesh of $41 \times 41 \times 41$ in the irreducible Brillouin zone. The energy convergence criterion is set as 10^{-6} Ry. Dynamical stability of these compounds is studied using PHONOPY code [21]. Heisenberg exchange coupling constants J_{ij} are calculated using Munich spin-polarized relativistic Korringa–Kohn–Rostoker (SPRKKR) package [22–24]. The scf calculations are carried with an angular momentum cut-off of $l_{max} = 3$ in the full-potential mode on a k-mesh of $22 \times 22 \times 22$ (578 points in the irreducible Brillouin zone) in scalar relativistic mode. The charge convergence has been further improved by employing Lloyds formula

for the Fermi energy determination [25,26]. Again the same generalized gradient approximation of Perdew, Burke and Ernzerhof [20] exchange–correlation potential were used here and the calculations are converged up to 0.1 meV. For Heisenberg exchange calculation, a k-mesh of $31 \times 31 \times 31$ with 1496 points in the irreducible Brillouin zone was taken. Disorder calculations are performed in SPRKKR using Coherent Potential Approximation (CPA).

2.2. Theoretical formulation

Mechanical stability and elastic properties are studied by calculating elastic constants. For cubic symmetry, there exists three independent elastic constants (i.e C_{11}, C_{12}, C_{44}). Born stability criteria [32] for the systems that crystallize in cubic structures are given by

$$C_{11} - C_{12} > 0, C_{11} + 2C_{12} > 0, C_{44} > 0 \quad (1)$$

If the Born stability criteria is satisfied, the compound is claimed to have mechanical stability. The elastic constant C_{11} is the longitudinal deformation, C_{12} is the stiffness and C_{44} is the transverse expansion. After computing elastic constants, the other elastic properties like anisotropic factor (A), Young's modulus (E), bulk modulus (B), shear modulus (G), Poisson's ratio (σ), have been calculated with Voigt–Reuss Hill approximation [33] using the standard empirical relations given as:

$$A = \frac{2C_{11}}{C_{11} - C_{44}} \quad (2)$$

$$E = \frac{9BG}{3BG + G} \quad (3)$$

$$G_V = \frac{3C_{44} + C_{11} - C_{12}}{5} \quad (4)$$

$$G_R = \frac{5(C_{11} - C_{12})C_{44}}{4C_{44} + 3(C_{11} - C_{12})} \quad (5)$$

$$B = \frac{(C_{11} + 2C_{12})}{3} \quad (6)$$

$$G_H = \frac{G_V + G_R}{2} \quad (7)$$

$$\sigma = \frac{(3B - 2G)}{2(3B + G)} \quad (8)$$

The spin polarization in a magnetic material can be found by knowing the contribution from the spin-up and spin-down states at the Fermi level. If $N \uparrow$ and $N \downarrow$ are the density of states at Fermi level E_F in majority and minority spin cases, then the degree of spin polarization P can be evaluated from the equation:

$$P = \frac{N \uparrow - N \downarrow}{N \uparrow + N \downarrow} \times 100 \quad (9)$$

Heisenberg exchange coefficients were computed for all the compounds using Munich spin-polarized relativistic Korringa–Kohn–Rostoker (SPRKKR) package. Exchange interactions among atoms are described in terms of classical Heisenberg exchange Hamiltonian which describes the magnetic exchange coupling as given by [34,35]

$$H_{eff} = - \sum_{\mu, \nu} \sum_{R, R'} J_{RR'}^{\mu\nu} S_R^\mu S_{R'}^\nu \quad (10)$$

where μ and ν represent different sublattices and R, R' denotes the lattice vectors of the atoms within the sublattices, S_R^μ denotes the unit vector pointing in the direction of the local magnetic moment at site (μ, R). We have employed real-space approach in order to calculate $J_{RR'}^{\mu\nu}$. For a multi-sublattice materials like Co_2CrX ($X = \text{Al}, \text{Ga}, \text{In}$), we need to use coupled equations [36]

$$\langle S^\mu \rangle = \frac{2}{3k_B T} \sum_{\nu} J_0^{\mu\nu} \langle S^\nu \rangle \quad (11)$$

$$J_0^{\mu\nu} = \sum_{R \neq 0} J_{0R}^{\mu\nu} \quad (12)$$

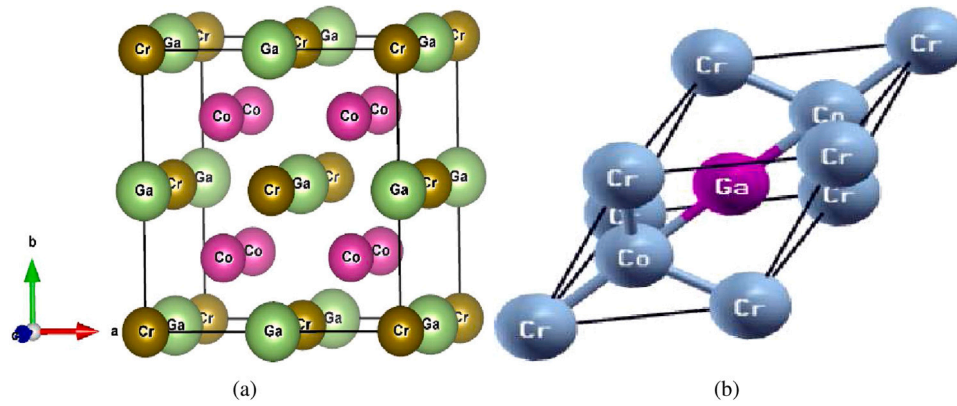


Fig. 1. The crystal structure of Co_2CrX ($X = \text{Al, Ga}$ and In) in (a) conventional and (b) primitive unit cells.

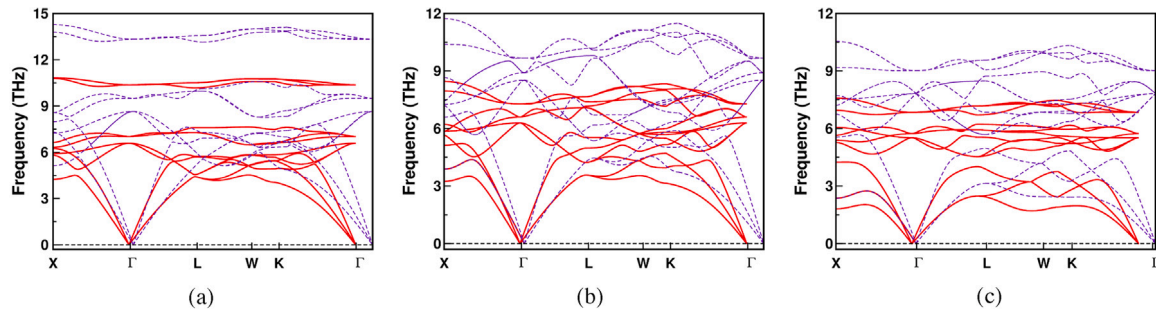


Fig. 2. The phonon dispersion relations of Co_2CrX ($X = \text{Al, Ga}$ and In) are shown respectively in (a, b, c). The solid lines represent ambient pressure $V/V_0 = 1.00$ and dashed lines represent $V/V_0 = 0.85$.

Table 1

Experimental and optimized lattice parameters, Magnetic moments and Curie temperature values of Co_2CrX , ($X = \text{Al, Ga, In}$) at ambient condition.

Compound	Lattice parameters (\AA)		Magnetic moment (μ_B)		Curie temperature (K)	
	Experiment	Calculated	Experiment	Calculated	Experiment	Calculated
Co_2CrAl	5.73 ^a	5.70	1.55 ^d	2.99	334 ^e	517.7
Co_2CrGa	5.80 ^b	5.71	3.01 ^d	3.02	495 ^f	466.5
Co_2CrIn	6.06 ^c	5.96	1.18 ^c	3.14	–	359.1

^aRef [27].

^bRef [28].

^cRef [29].

^dRef [30].

^eRef [31].

^fRef [28].

where $\langle S^z \rangle$ is the average z-component of S_R^z and $J_0^{\mu\nu}$ represents the effective exchange interactions in the sublattices μ and ν . The summation R in Eq. (12) was taken up to a radius of $R_{max} = 4.5a$, where ‘ a ’ is a lattice constant. This can be represented in the eigen value matrix problem as follows:

$$(\Theta - TI)S = 0 \quad (13)$$

where $\Theta_{\mu\nu} = (\frac{2}{3}k_B)J_0^{\mu\nu}$, I is the unit matrix, $S = \langle s^z \rangle$ and the largest eigen value of the matrix Θ gives Curie temperature.

3. Results and discussion

3.1. Ground state and magnetic properties at ambient conditions

The ground state electronic and magnetic properties of Co-based Heusler compounds Co_2CrX ($X = \text{Al, Ga}$ and In) are investigated. Previous studies on Co_2CrX ($X = \text{Al, Ga}$ and In) predict the possibility of two atomic position arrangements for Cr and X atoms where, in the first arrangement Cr atom is located at (0,0,0) position and X atom is located

at (1/2, 1/2, 1/2), and in the second arrangement the atomic position of Cr and X atoms are swapped [37,38]. Our total energy calculations confirm that, the theoretical ground state of Co_2CrAl and Co_2CrGa are observed in first configuration and the ground state of Co_2CrIn is found to be in second configuration. Crystal structure of the studied compounds in conventional and primitive unit cells is shown in Fig. 1(a, b). Further, the ferromagnetic ground state of all the compounds is confirmed using spin polarized calculations. Computed ground state properties of all the studied compounds along with the experimentally reported values are given in Table 1. From Table 1, it is clear that, the theoretically optimized values are in reasonable agreement with experimental ones. The total magnetic moments obtained for the three compounds Co_2CrX ($X = \text{Al, Ga}$ and In) are $3.00\mu_B$, $3.02\mu_B$ and $3.14\mu_B$ respectively. The partial magnetic moment of Co is $0.82\mu_B$, $0.78\mu_B$, $0.726\mu_B$ and that of Cr is $1.43\mu_B$, $1.49\mu_B$, $1.71\mu_B$ for the three compounds respectively. All the calculated magnetic moments are in agreement with the Slater–Pauling rule. According to Slater Pauling rule, the magnetic moment is given by,

$$m = N_v - 24$$

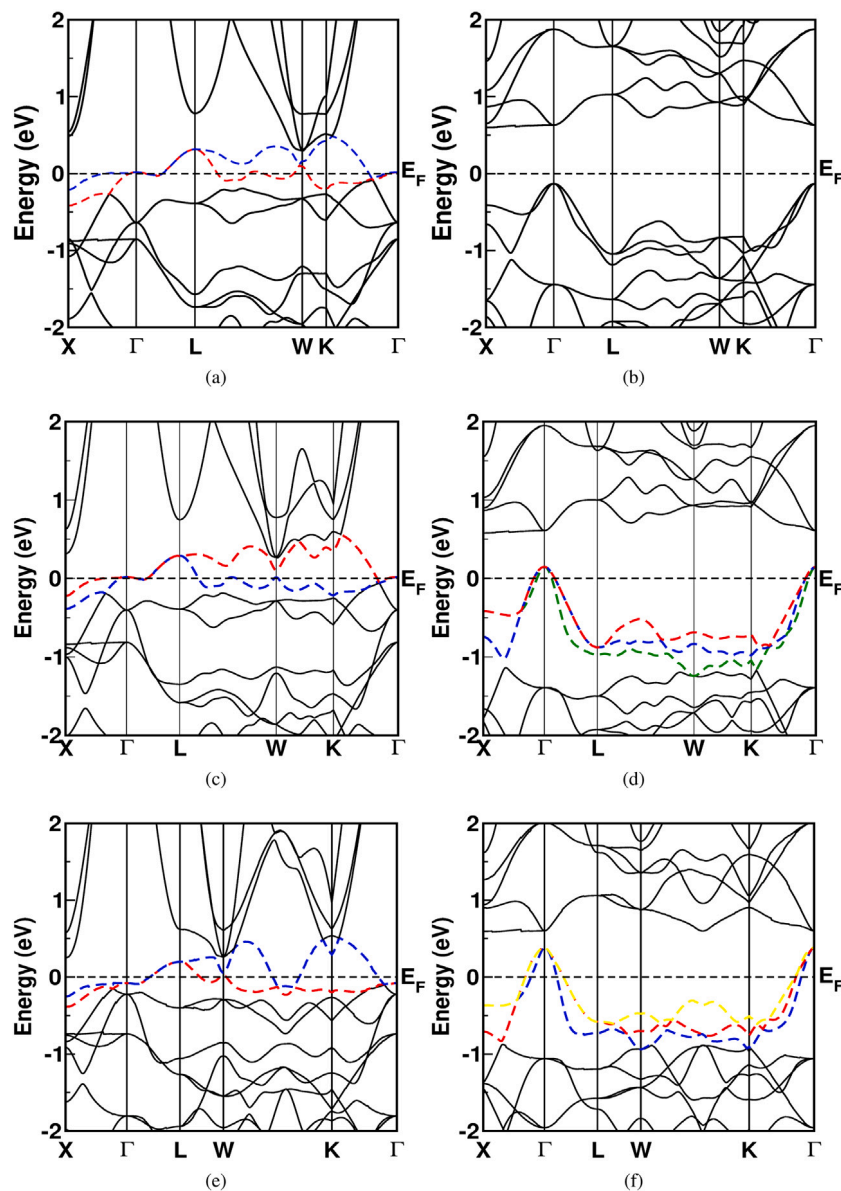


Fig. 3. The majority and minority spin bandstructures for Co_2CrAl in (a, b), Co_2CrGa in (c, d) and Co_2CrIn in (e, f) compounds at ambient pressure $V/V_0 = 1.00$.

where, N_v is the number of valence electrons in the compound. In all the three compounds, there are 27 valence electrons. Therefore, the expected magnetic moment should be $3\mu_B$ for all the compounds, and for Co_2CrGa , our theoretical results are in good agreement with the experimental data. But in case of Co_2CrAl and Co_2CrIn , the experimental and the obtained magnetic moments differ with each other. The generalized gradient approximation (GGA) to the exchange–correlation potential of Perdew–Burke–Ernzerhof parametrization, which is used here often does not predict exact band gap. This issue stems from the fact that GGA relies completely on the local electronic density and its gradient. However, an accurate description requires more information. One such milestone work, which describes the accuracy limitations of standard DFT is given by Pople and co-workers [39]. Coming to the family of Co-based Heusler compounds, such as Co_2CrAl , we always find the magnetic moment computed from DFT to differ from the experiments [40,41]. The work by Kandapal et al. which is cited here, has also included the correlation effects through LSDA+U and the studies still could not resolve the difference found between the experimental and theoretical magnetic moment values. Our calculation with GGA+U is in agreement with earlier work and magnetic moment is larger than

the experimental value. So, the possible reason for the above mentioned discrepancy may be due to the antisite disorder present in the experiments which eventually decreases the magnetic moment when compared to the ordered state calculation. Recent calculations [41] show that 37% disorder is approximately required in order to achieve the $1.6\mu_B$ observed experimentally. This could also be one of the reasons for the observed deviations, in addition to the exchange correlation functional. To check this, D03-type [41] disorder calculations are performed on Co_2CrAl and Co_2CrIn compounds at ambient conditions. The obtained magnetic moments for Co_2CrAl and Co_2CrIn are $1.7\mu_B$ and $1.1\mu_B$ respectively for 27%-disorder and 30%-disorder which are in close agreement with experimental magnetic moments of both the compounds, further supporting the presence of disorder causing the suppression of magnetic moments in these compounds. This can be verified from the earlier experimental reports [42,43] which show that the disorder tends to reduce magnetization, spin polarization and may eventually result in lower Curie temperature.

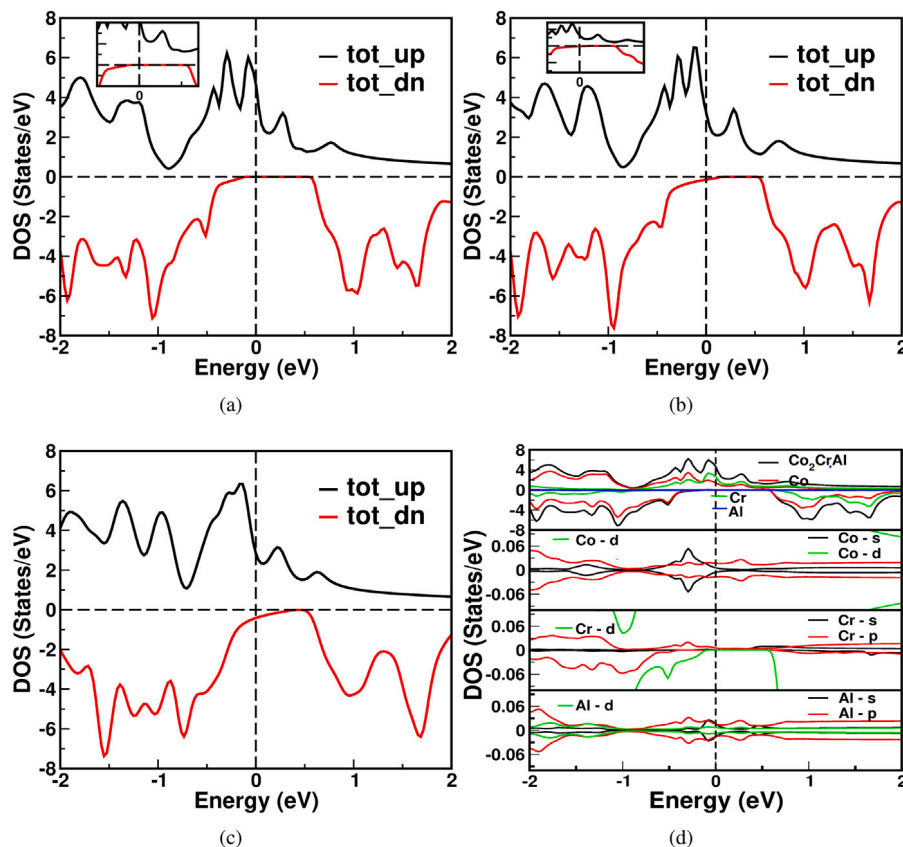


Fig. 4. The total density of states for Co_2CrAl , Co_2CrGa , Co_2CrIn in (a, b, c) and Partial DOS of Co_2CrAl at ambient pressure $V/V_0 = 1.00$ in (d) respectively.

3.2. Mechanical and dynamical stability at ambient condition

The elastic constants of these three systems are studied at the ambient condition and it is found that, these constants satisfy the Born stability criteria given in Eq. (1) confirming the mechanical stability of the system. It should also be noted that, the Born stability criteria is based on harmonic approximation and cannot account for the metastable state. All the investigated compounds are found to be anisotropic which implies that the mechanical properties of the solids will differ in different directions. The value of shear modulus G is found to be highest for Co_2CrAl and lowest for Co_2CrIn in the series of Co_2CrX ($X = \text{Al}$, Ga and In) at the ambient condition. From the obtained bulk moduli B for the studied compounds, it is found that the compound Co_2CrGa has the highest resistance to fracture. Young's modulus E of a material indicates the ratio of linear stress to linear strain. Young's modulus is highest for the compound Co_2CrAl and is lowest for Co_2CrIn . At the ambient conditions, all the three compounds are found to be ductile since the value of $B/G > 1.75$. All the elastic properties of the compounds are provided in Table 2.

As a next step, we have calculated phonon dispersion to check the dynamical stability of the investigated systems. The number of vibrational modes in primitive cell of all the compounds were 12. The phonon dispersion curves has acoustic modes and optical modes. There will be 3 acoustic modes and $(3N - 3)$ optical modes present in which, N is the number of atoms per unit cell. The phonon band structure of compounds Co_2CrX ($X = \text{Al}$, Ga and In) is plotted in Fig. 2(a, b, c). From Fig. 2, it is found that the three low frequency modes are acoustic in nature and the remaining nine branches are the optical modes. From the same plots, the absence of the imaginary frequencies in phonon dispersion confirm the dynamical stability of the systems investigated. Maximum phonon frequency is found to decrease from Co_2CrAl to Co_2CrIn which might be due to the large mass of

Table 2

Single crystalline elastic properties of Co_2CrX ($X = \text{Al}$, Ga and In) at ambient pressure. Here C_{11}, C_{12}, C_{44} are the elastic constants in GPa, A is anisotropic factor, G is shear modulus in GPa which is the average of G_v and G_R shear moduli calculated using Voigt and Reuss approximations respectively, B is bulk modulus in GPa, E is Young's modulus in GPa, σ is Poisson's ratio and P_c is Paugh's ratio and C_s is the effective shear modulus.

Parameter	Co_2CrAl	Co_2CrGa	Co_2CrIn
C_{11} (GPa)	266.54	332.59	213.44
C_{12} (GPa)	169.56	250.64	152.39
C_{44} (GPa)	142.98	145.91	95.44
A	2.95	3.56	3.13
G_V (GPa)	105.18	103.94	69.47
G_R (GPa)	80.34	72.08	51.57
B (GPa)	201.89	277.96	172.74
G (GPa)	92.77	88.01	60.52
E (GPa)	241.33	238.81	162.58
B/G	2.18	3.16	2.85
σ	0.3	0.36	0.34
$P_c = C_{11} - C_{12}$	96.96	81.94	61.06
$C_s = (C_{11} - C_{12})/2$	48.48	40.97	30.53

Indium. The frequency difference between the optical modes is largest for Co_2CrAl which may be attributed to the differences in masses of atoms in that compound while the frequency gap between the optical modes for the other compounds are quite less as can be evidenced from Fig. 2. In the present work, both mechanical and dynamical stability calculations are performed under harmonic approximation, which gives a global local minima of the system at OK. This approach has limitations, where entropy contributions are completely neglected and this can be achieved by the technique called metadynamics as reported earlier by Alessandro Barducci et al. [44], but it should be mentioned that it is computationally too expensive and beyond the scope of present work.

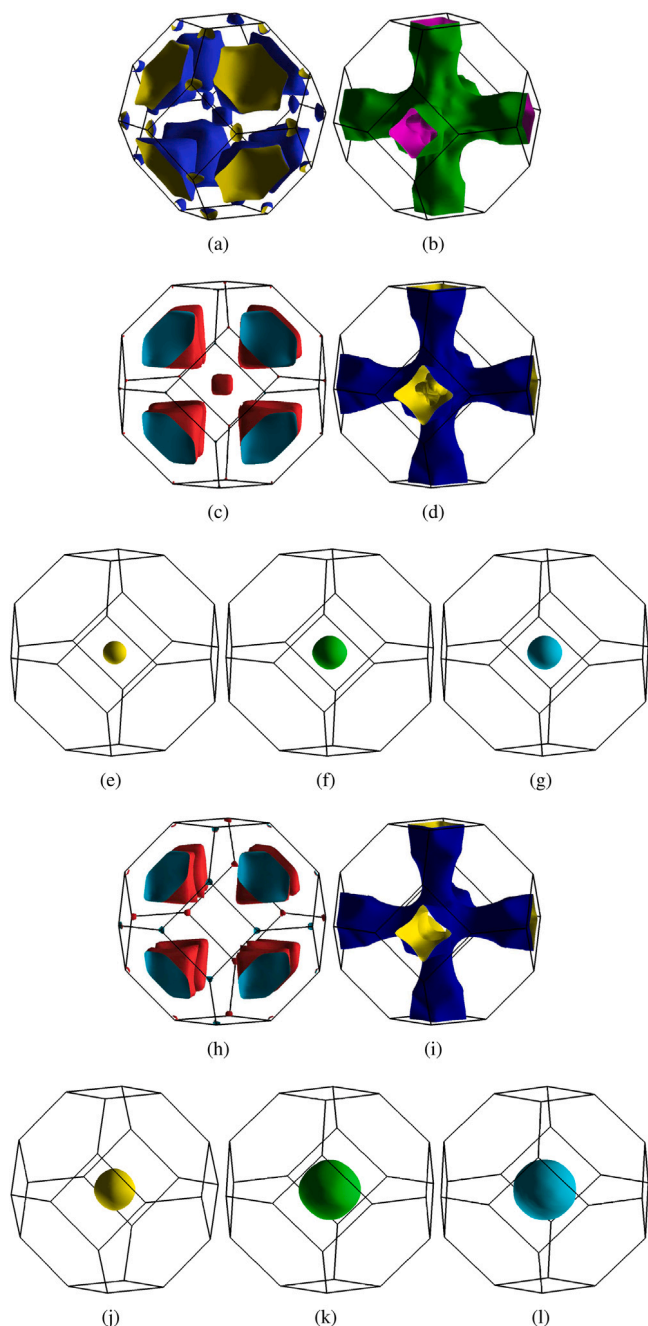


Fig. 5. The Fermi surface topology of Co_2CrAl in (a, b), for Co_2CrGa in (c, d) and for Co_2CrIn (h, i) for majority spin case and FS topology for compounds Co_2CrGa in (e, f, g) and for Co_2CrIn in (j, k, l) for minority spin cases respectively at ambient pressure when $V/V_0 = 1.00$.

3.3. Band structure and Fermi surface topology

In Fig. 3, we have provided the spin polarized band structure of Co_2CrX ($X = \text{Al, Ga and In}$). The analysis of band structure of Co_2CrAl shows that the compound is half metallic as only majority spin case (i.e spin-up) shown in Fig. 3(a) is conducting while the minority spin case (spin-down) is reported as semiconductor as shown in Fig. 3(b). It is to be mentioned that the standard DFT-PBE functionals are well known to underestimate the band gap of solids and this can be rectified by using the TB-mBJ functional as implemented in Wien2k [45,46]. In case of Co_2CrAl , the half-metallic gap is found to increase from 0.73 eV to 1.34 eV by employing TB-mBJ functional. In majority spin case, two

bands are crossing the E_F from the valence band to the conduction band indicating that these two bands are hole-type in nature. The overlapping of these two bands near E_F is observed around Γ , L, W and K high symmetry points which are shown in Fig. 3(a) and the corresponding Fermi surface (FS) topology is shown in Fig. 5. (a, b). The derived Fermi surfaces are found to be different. In the case of first FS, around L point, a cone like envelope is observed directed towards Γ - point and a small curved sheet around W-point. In the case of second Fermi surface, a cylindrical shape pocket is observed around X-point, and all these pockets are found to be connected through the center of the Brillouin zone. The band structure of the compound Co_2CrGa is shown in Fig. 3(c, d) where it can be seen that the compound is nearly half metallic as majority spin channel is conducting with two bands crossing the E_F , while the minority spin channel is also slightly conducting with three bands crossing near the E_F around Γ -point. For Co_2CrGa , the FS topology for majority spin case are shown in Fig. 5 (c, d) and for minority spin case in Fig. 5(e, f, g). Here, the FS of spin-up states are in line with Co_2CrAl , spin-down FS are found to be in spherical shape around Γ - point. The band structure analysis of Co_2CrIn suggests that Co_2CrIn is not a half metal as both majority and minority spin channels have significant conductivity. Two bands are found to cross E_F in majority spin case and corresponding FS topology is shown in Fig. 5(h, i), while three bands are crossing E_F in minority spin case as seen from Fig. 3(e, f) and the corresponding FS topology is shown in Fig. 5(j, k, l).

3.4. Density of states and degree of spin polarization

Understanding of total and partial density of states in general provides a better picture of the electronic structure and they are shown in Fig. 4 for Co_2CrX ($X = \text{Al, Ga and In}$) compounds. From Fig. 4(a), it is clear that the compound Co_2CrAl is a half metal as the DOS near E_F is zero for one spin channel. The compound Co_2CrGa possesses nearly half metallic character as can be seen from Fig. 4(b) while the compound Co_2CrIn possesses metallic character which is evidenced from Fig. 4(c). In case of Co_2CrX ($X = \text{Al, Ga and In}$), the major contribution near Fermi level E_F is coming from the Cr-d states as can be seen from the atom projected density of states for Co_2CrAl shown in Fig. 4(d). So, understanding the magnetic exchange interaction between Cr and Co atoms is important in these three compounds which are discussed in the next section. From the total density of states calculations, the total DOS in majority and minority spin cases $N \uparrow$ and $N \downarrow$ are calculated. Using both $N \uparrow$ and $N \downarrow$, the degree of spin polarization P is calculated using Eq. (9). The degree of spin polarization P obtained for the compounds Co_2CrX ($X = \text{Al, Ga and In}$) are respectively 100%, 91.81% , 71.20% at ambient which enable them as potential candidates in spintronic applications because of high spin polarization.

3.5. Magnetic exchange interactions

To investigate the strength of the magnetic interactions among the various atoms in Co_2CrX ($X = \text{Al, Ga and In}$) compounds, the Heisenberg exchange interaction J_{ij} has been plotted as a function of R_{ij}/a where J_{ij} represents the Heisenberg exchange constant between the sites i and j , R_{ij} is the nearest neighbor distance and 'a' is the lattice parameter of the compound. The strength of the magnetic interaction is determined by the exchange constants J_{ij} . The positive values of J_{ij} indicate ferromagnetic (FM) coupling between the atoms and negative values indicate the antiferromagnetic (AFM) coupling between the atoms. Variation of exchange coupling parameter J_{ij} with R_{ij}/a and first four nearest neighbors as a function of V/V_0 for different compressions corresponding to $V/V_0 = 1.00, 0.95, 0.90$ and 0.85 is shown for Co_2CrAl in Fig. 11(a, b) and respectively.

In Co_2CrAl , for the ambient condition $V/V_0 = 1.00$, it is evident that Co_1/Co_2 -Cr and Co_1 - Co_2 interactions are dominating. Out of these two interactions, the highest value of exchange coupling constant (J_{ij}) is for

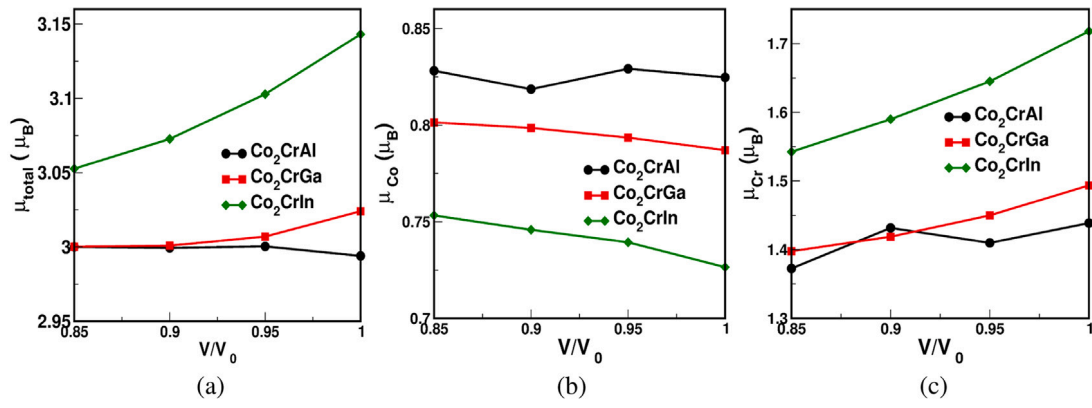


Fig. 6. The variation of total magnetic moment (μ_B) in (a), Co moment (μ_B) in (b) and Cr moment (μ_B) in (c) respectively as a function of V/V_0 .

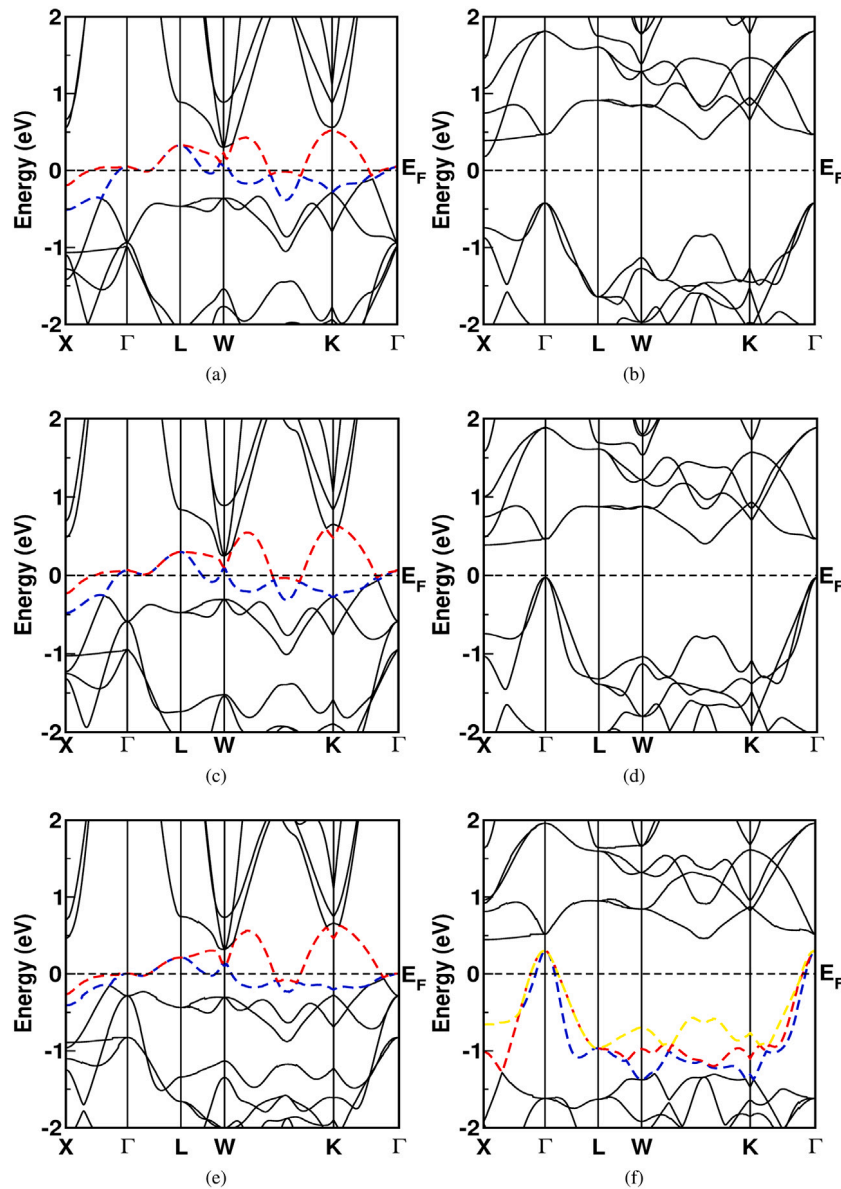


Fig. 7. The majority and minority spin bandstructures for Co_2CrAl in (a, b), for Co_2CrGa in (c, d) and for Co_2CrIn in (e, f) respectively at $V/V_0 = 0.85$.

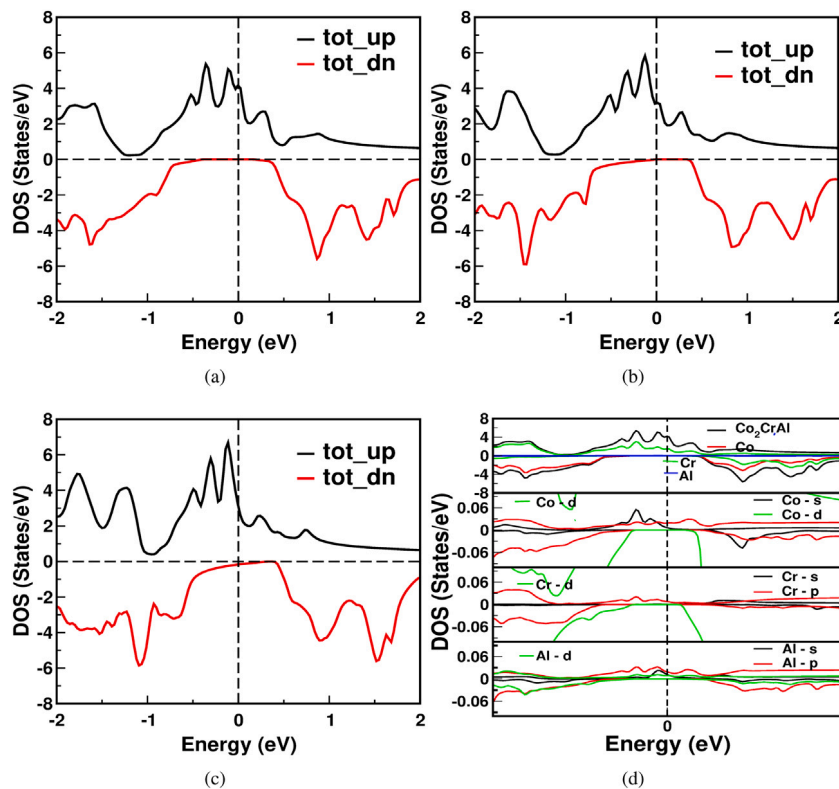


Fig. 8. The total density of states for Co_2CrAl , Co_2CrGa , Co_2CrIn in (a, b, c) and Partial DOS of Co_2CrAl at $V/V_0 = 0.85$ in (d) respectively.

Co_1/Co_2 -Cr indicating that magnetic strength between Co_1/Co_2 and Cr is the strongest among all interactions and that the interaction is most FM in nature. The strongest interactions reflect the nearest distance between the respective atoms. This is also verified by checking the distances between all the atoms, and that Cr is the nearest neighbor to Co with a value of 2.48 Å. The first nearest neighbor interactions in both Co_1 - Co_1 and Cr-Cr are AFM in nature and the second nearest neighbor interactions are FM in nature. This type of oscillating behavior between FM and AFM coupling is attributed to the Ruderman-Kittel-Kasuya-Yosida (RKKY)-type interactions. The interactions of Co/Cr with Al and Al-Al are nearly zero for all the distances and hence are not shown in figure. Though there is a competition between FM and AFM states in this compound due to RKKY-type interaction, ultimately FM interactions dominate over AFM interactions and hence the compound remains FM in nature. A similar trend is observed for Co_2CrGa and Co_2CrIn and hence they are not shown here and they are also FM in nature. But for Co_2CrIn , Co_1 (Co_2)- Co_1 (Co_2) and Cr-Cr interactions are AFM in nature in terms of first and second nearest neighbor distances. But the compound is FM in nature due to the dominating nature of positive J_{ij} for $\text{Co}_1/(\text{Co}_2)$ -Cr and Co_1 - Co_2 interactions. The calculated Curie temperature T_C from mean field approximation along with experimental T_C values for these compounds at ambient are given in Table 1. We can observe that, the theoretically calculated values of T_c are in reasonable agreement with experimental values, which may be due to the inherent limitation of Exchange correlation functionals used to compute the exchange coupling parameters J_{ij} .

4. Strain effects

The changes in the Fermi surface topology such as the cross-sectional area, curvature and shape are directly related to the changes in physical properties of metals as FS topology explains the physical properties of the metallic systems. The variation of the Fermi surface topology induces changes at some particular points due to the application of thermal, chemical or hydrostatic pressure, due to which there

might be a change in behavior in elastic, thermodynamic and transport properties [47]. These changes in FS topology may lead to Electronic Topological Transitions (ETTs) [48]. The authors [49,50] in their study have reported the magnetic to non-magnetic transition under external pressure and they connected this transition to ETTs. A transition from pure half-metallic state to nearly half-metallic state is reported in quaternary heusler alloy CoRuFeSi [51], while the authors have reported a phase transition from semimetallic cubic phase to a likely semimetallic tetragonal phase in semiheusler compound CuMnSb [52]. So by applying the external pressure in the form of compressive strain to our compounds Co_2CrX ($X = \text{Al, Ga, In}$), the changes in FS topology and hence the possibility ETTs are discussed.

To explore the percentage of spin polarization and possibility of electronic topological transitions as a function of strain, the hydrostatic compressive strain is applied to the investigated Co_2CrX ($X = \text{Al, Ga}$ and In) compounds. The compounds Co_2CrX ($X = \text{Al, Ga}$ and In) are subjected to a volume compression of $V/V_0 = 0.95, 0.90$ and 0.85 respectively with a step size of $V/V_0 = 0.05$ and the corresponding changes in the magnetic, mechanical, electronic and FS topology and spin polarization of these systems under compressive strain are discussed in the following sections.

The variation of magnetic moment of Co_2CrX ($X = \text{Al, Ga}$ and In) compounds under compression are shown in Fig. 6. It is clear from Fig. 6(a) that the total magnetic moment almost remains same for Co_2CrAl , while it decreases for Co_2CrGa and Co_2CrIn compounds with V/V_0 . The magnetic moment of Co atom increases with V/V_0 for Co_2CrGa and Co_2CrIn compounds while it shows non-monotonic variation for Co_2CrAl as can be seen from Fig. 6(b). Similarly, the magnetic moment of Cr atom decreases with V/V_0 for Co_2CrGa and Co_2CrIn compounds while it shows non-monotonic variation for Co_2CrAl as can be seen from Fig. 6(c).

In case of Co_2CrAl , the band profiles at the ambient and at the strained states remain same which can be evidenced from Fig. 7(a, b). When compressive strain is applied, the Fermi level E_F is shifted upwards. The compound retains its half-metallicity even up to the

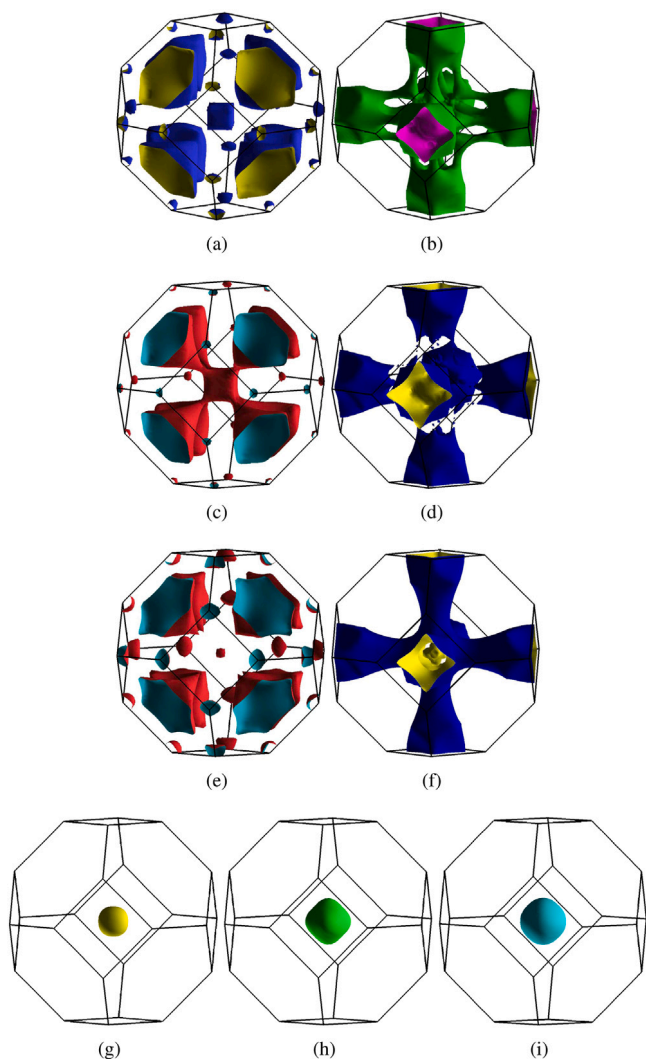


Fig. 9. The Fermi surface topology of Co_2CrAl , Co_2CrGa and Co_2CrIn in (a, b), (c, d) and (e, f) for majority spin case and FS topology for compound Co_2CrIn in (g, h, i) for minority spin case at $V/V_0 = 0.85$.

maximum studied compression around $V/V_0 = 0.85$ (48 GPa). This is verified in the behavior of DOS plot at the Fermi level (i.e the total DOS at Fermi level is zero in spin-down channel) from Fig. 8(a). At the ambient condition, there is a hole pocket along the high symmetry points Γ , L, W and along $X-\Gamma$ while in the strained state at $V/V_0 = 0.85$, the size of the hole pocket along $X-\Gamma$ increases. Also, one can observe that the overlapping around Γ is found to increase in the strained state at $V/V_0 = 0.85$ which can be observed through FS topology from Fig. 9(a, b). A slight change in the FS topology is visualized as an electronic topological transition (ETT) and the corresponding FS topology which undergoes a topology change is shown in Fig. 9(a, b). In the case of Co_2CrGa , two bands are found to cross from the valence band to the conduction band at the ambient condition in minority spin case shown in Fig. 3(d). With the application of compressive strain at $V/V_0 = 0.85$ (44 GPa), these two band crossings have disappeared and the minority spin channel becomes semiconducting, which is shown in Fig. 7(d). Since there is a change in the FS topology at $V/V_0 = 0.85$ due to application of strain, and hence one can see an Electronic topological transition (ETT) at $V/V_0 = 0.85$. Thus an electronic topological transition (ETT) which is visualized, drives the half-metallicity at the compression corresponding to $V/V_0 = 0.85$ and the corresponding FS is shown in Fig. 9 (c, d). For Co_2CrIn , we observe the change in

band profile along $X-\Gamma$ and at W in majority spin channel at ambient (Fig. 3(e, f)) and under compression corresponding to $V/V_0 = 0.85$ (74 GPa) (Fig. 7(e, f)). This leads to an ETT and the changed FS are shown in Fig. 9(e, f) in spin up channel. A small decrease can be seen in the size of the hole pocket in the minority spin case around a compression of $V/V_0 = 0.85$ which is further evidenced by FS topology as shown in Fig. 9(g, h, i). In the case of majority spin, the band overlap along $X-\Gamma$ and $L-\Gamma$ is found to increase which may induce change in the FS topology. At $V/V_0 = 0.85$, the overall profile looks same but the size of the hole pocket at Γ -point has reduced in minority spin case.

The density of states of Co_2CrX ($X = \text{Al, Ga and In}$) compounds at $V/V_0 = 0.85$ is shown in Fig. 8. It is obvious from Fig. 8(a) that the compound Co_2CrAl retains half metallic character, while from Fig. 8(b) the compound Co_2CrGa becomes half metallic due to ETT. For Co_2CrIn at $V/V_0 = 0.85$, it still shows metallic character as shown Fig. 8(c). The variation of degree of spin polarization P with V/V_0 is shown in Fig. 12(b). The degree of spin polarization P of Co_2CrAl remains 100% with V/V_0 which may be due to half metallicity, while it increases for both Co_2CrGa and Co_2CrIn compounds which may be due to ETT as a function of pressure and spin polarization reaches 100% for Co_2CrGa .

The mechanical stability of these systems again verified by Born stability criteria as given in Eq. (1) and all the compounds under different strains (V/V_0 values) satisfy it. The variation of elastic constants C_{11} , C_{12} , C_{44} and effective shear modulus $C_s = (C_{11} - C_{12})/2$ of Co_2CrX ($X = \text{Al, Ga and In}$) as a function of volume V_0 is plotted in Fig. 10. It is clear from Fig. 10 that all the C_{ij} and C_s increase as V/V_0 goes from 1.00 to 0.85. Also, it is observed that the elastic moduli bulk modulus B, Young's modulus E, and Shear modulus G gradually increase under compression. All the investigated compounds are found to be anisotropic as the value of anisotropy factor A is not equal to unity for all the compounds under compression. The Pugh's ratio B/G reveals that all the compounds under all compressions are brittle in nature. As the value of Poisson's ratio is within 0.30 to 0.37, for all the compounds under compression, the inter-atomic forces will be central forces. The absence of imaginary frequencies in all the compounds for $V/V_0 = 0.85$ as shown in Fig. 2(a, b, c) indicate that these compounds are also dynamically stable under compression.

The Heisenberg magnetic exchange coupling constants J_{ij} are calculated for all Co_2CrX ($X = \text{Al, Ga and In}$) compounds and here we have presented the details at different V/V_0 values and the variation of exchange interactions for the first four nearest neighbor distances (NN) among the atoms as a function of V/V_0 is shown in Fig. 11(a, b) for Co_2CrAl . For Co_2CrAl , which is shown in Fig. 11(a, b), it is clear that Co-Cr, $\text{Co}_1\text{-Co}_2$ and Co-Co interactions increase continuously up to the value $V/V_0 = 0.85$, where ETT is evidenced. The Cr-Cr interactions are more negative initially and become positive with $V/V_0 = 0.85$. The same explanation can be given for the other two compounds. Hence the details of the other two compounds are not shown here. All the three compounds still possess ferromagnetic nature until the maximum studied compression as evidenced from overall positive J_{ij} 's. Similarly, the variation in Curie temperature T_C as a function of V/V_0 is shown in Fig. 12(a). For all Co_2CrX ($X = \text{Al, Ga and In}$) compounds, the T_C increases continuously as a function of V/V_0 till 0.85, which can be verified with the behavior of J_{ij} under compressions and the maximum Curie temperature is found to be 646.1 K for Co_2CrAl under compression corresponding to $V/V_0 = 0.85$.

5. Conclusion

The effect of spin polarization under the application of compressive strain has been studied for the compounds Co_2CrX ($X = \text{Al, Ga and In}$). The percentage of spin polarization is found to increase for all the compounds Co_2CrX ($X = \text{Al, Ga and In}$) with compressive strain. Among the present studied compounds, Co_2CrGa , which is nearly half metallic in nature at ambient pressure attains half-metallicity at compression corresponding to $V/V_0 = 0.85$ with 100% spin polarization. The strain

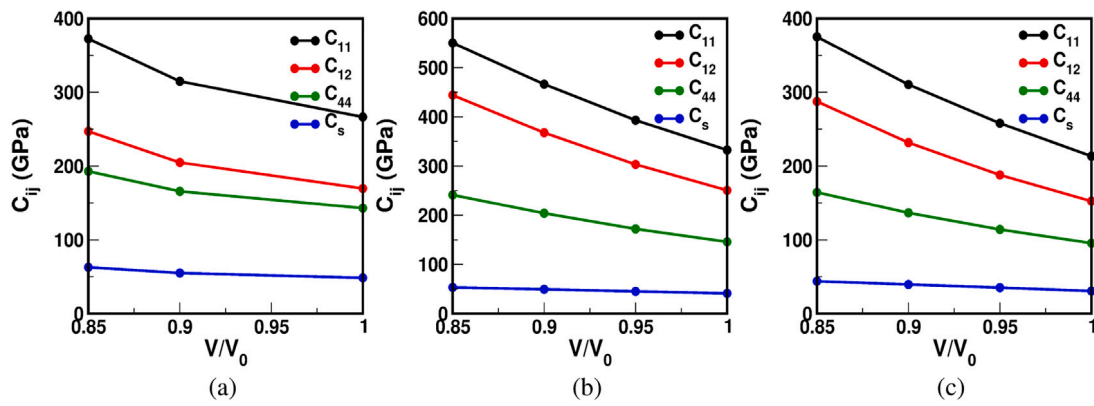


Fig. 10. The variation of elastic constants C_{11} , C_{12} , C_{44} and $C_s = (C_{11} - C_{12})/2$ as a function of V/V_0 for Co_2CrX , (X = Al, Ga and In) shown in (a, b, c) respectively.

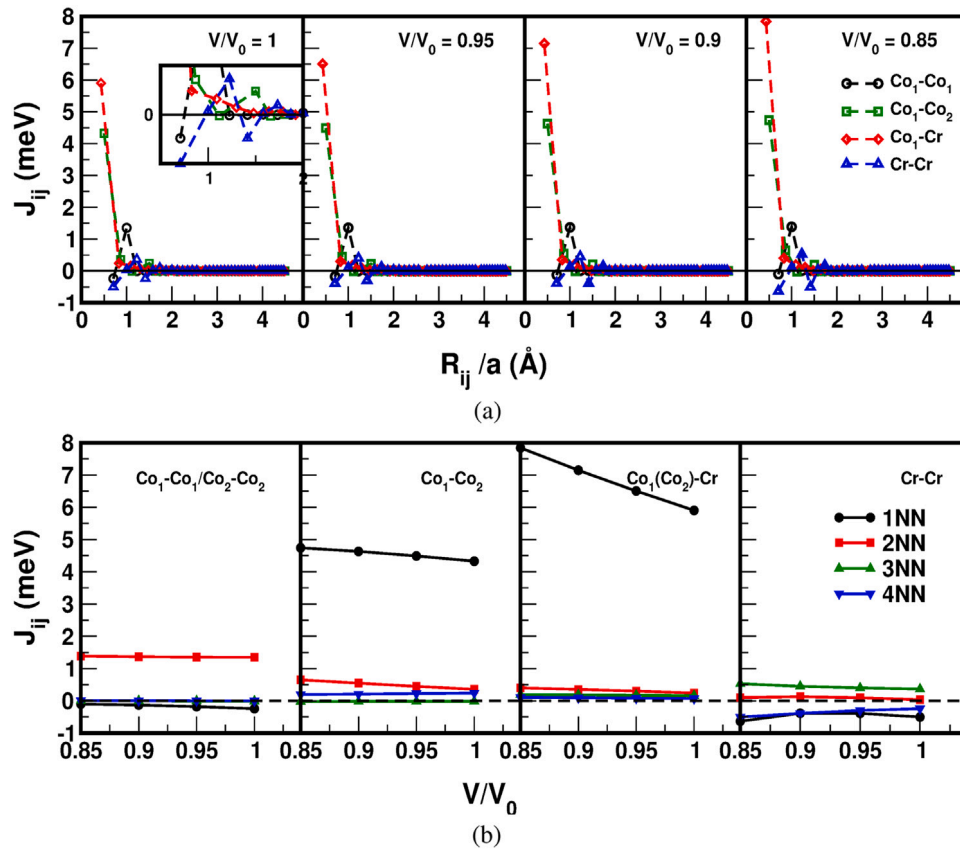


Fig. 11. (a) The variation of Heisenberg exchange interactions as a function of R_{ij}/a for different V/V_0 values. (b) The variation of J_{ij} of different nearest neighbor interactions as a function of V/V_0 for Co_2CrAl .

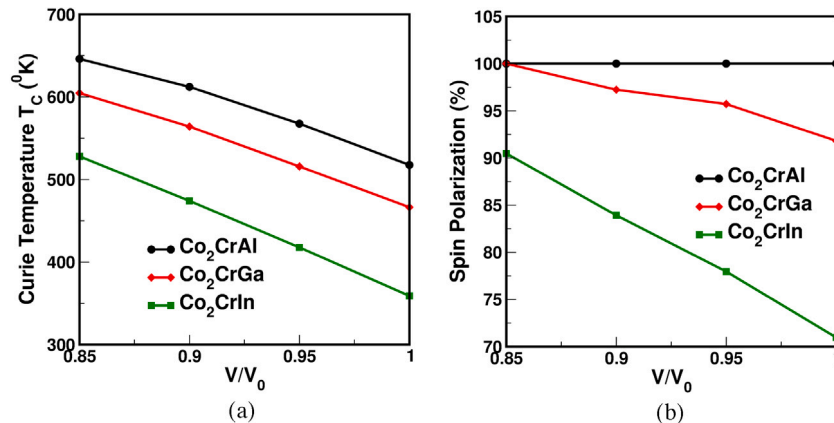


Fig. 12. The variation of Curie temperature T_c in (a) and the percentage of spin polarization in (b) as a function of V/V_0 .

induced enhanced spin polarization may be helpful for spintronic applications. An Electronic Topological Transition (ETT) is observed mainly in Co_2CrGa compound which is responsible for its half-metallicity under compression corresponding to $V/V_0 = 0.85$ whereas in other compounds, there exists a possibility of ETT at compression corresponding to $V/V_0 = 0.85$ due to the change in Fermi surface topology. The studied compounds are ferromagnetic in nature at ambient and under compression and is explained by the Heisenberg exchange interactions among the atoms, which reveals that the strong Co-Cr interaction is responsible for the ferromagnetic nature in these compounds. Also, the Curie temperature increases as function of V/V_0 which can be verified from the trend in exchange interactions J_{ij} as a function of R_{ij}/a and reaches a maximum value of 646.1 K for Co_2CrAl under compression corresponding to $V/V_0 = 0.85$.

CRedit authorship contribution statement

P. Rambabu: Investigation, Methodology, Writing - original draft.
B. Anuroopa: Investigation, Methodology, Writing - original draft.
M. Manivel Raja: Conceptualization, Investigation, Project administration, Supervision, Visualization, Writing - review & editing.
V. Kanchana: Conceptualization, Software, Methodology, Validation, Visualization, Project administration, Writing - review & editing.

Declaration of competing interest

The authors declare that they have no known competing financial interests or personal relationships that could have appeared to influence the work reported in this paper.

Acknowledgments

The authors PR, BA and VK would like to thank IIT Hyderabad for computational facility. PR, BA and VK would like to thank CDAC and DRDO project with Reference number (ERIP/ER/201701001/M/01/-1711) for computational facility. PR would like to acknowledge Guru Ghasidas Vishwavidyalaya, Bilaspur, Chhattisgarh for sponsoring the Ph.D. program. BA would like to acknowledge DST-INSPIRE for fellowship.

References

- [1] Igor Žutić, Jaroslav Fabian, S. Das Sarma, *Rev. Modern Phys.* 76 (2004) 323.
- [2] S. Palchoudhury, K. Ramasamy, A. Gupta, *Mater. Matters* 11 (2016) 4.
- [3] B. Balke, S. Wurmehl, G.H. Fecher, C. Felser, J. Küler, *Sci. Technol. Adv. Mater.* 9 (2008) 014102.
- [4] B. Parveen, Mahmood-ul Hassan, Z. Khalid, S. Riaz, S. Nasee, *J. Appl. Res. Technol.* 15 (2017) 132–139.
- [5] X. Li, J. Yang, *Nat. Sci. Rev.* 3 (2016) 365–381.
- [6] A. Hirohata, H. Sukegawa, H. Yanagihara, I. Žutić, T. Seki, S. Mizukami, R. Swaminathan, *IEEE Trans. Magn.* 51 (2015) 0800511.
- [7] M. Ramudu, M. Manivel Raja, J. Arout Chelvane, S.V. Kamat, *J. Magn. Magn. Mater.* 418 (2016) 42–47.
- [8] M. Ramudu, M. Manivel Raja, H. Basumatary, S.V. Kamat, *J. Magn. Magn. Mater.* 490 (2019) 165528.
- [9] A. Rajanikanth, Y.K. Takahashi, K. Hono, *J. Appl. Phys.* 103 (2008) 103904.

- [10] M.N. Rasul, A. Javed, M.A. Khan, A. Hussain, *Mater. Chem. Phys.* 222 (2019) 321–332.
- [11] Y. Srivastava, S.K. Vajpai, S. Srivastava, *J. Magn. Magn. Mater.* 433 (2017) 141–147.
- [12] V.K. Jain, V. Jain, N. Lakshmi, A.R. Chandra, K. Venugopalan, *Comput. Mater. Sci.* 108 (2015) 56–61.
- [13] K. Özdoğan, I. Galanakis, B. Aktaş, E. Şaşıoğlu, *J. Appl. Phys.* 101 (2018) 073910.
- [14] S. Amari, F. Dahmane, S.B. Omran, B. Doumi, I.E. Yahiaoui, A. Tadjer, R. Khenata, *J. Korean Phys. Soc.* 69 (2016) 1462–1468.
- [15] I. Galanakis, K. Özdoğan, B. Aktaş, E. Şaşıoğlu, *Appl. Phys. Lett.* 89 (2006) 042502.
- [16] Z. Gercsi, K. Hono, *J. Phys.: Condens. Matter* 19 (2007) 326216.
- [17] R.A. de Groot, F.M. Mueller, P.G. van Engen, K.H.J. Buschow, *Phys. Rev. Lett.* 50 (1983) 2024.
- [18] P. Blaha, K. Schwarz, P. Sorantin, S.B. Tricky, *Comput. Phys. Comm.* 59 (1990) 399–415.
- [19] F. Birch, *Phys. Rev.* 71 (1947) 809.
- [20] J.P. Perdew, K. Burke, M. Ernzerhof, *Phys. Rev. Lett.* 77 (1996) 3865–3868.
- [21] A. Togo, I. Tanaka, *Scr. Mater.* 108 (2015) 1–5.
- [22] H. Dreyse, *Electronic Structure and Physical Properties of Solids: The Use of the LMTO Method*, vol. 535, Springer-Verlag Berlin Heidelberg edition, 1998.
- [23] H. Ebert, J. Minár, V. Popescu, *Magnetic dichroism in electron spectroscopy*, in: K. Baberschke, W. Nolting, M. Donath (Eds.), *Band-Ferromagnetism*, in: *Lecture Notes in Physics*, vol. 580, Springer, Berlin, Heidelberg, 2001, pp. 371–385.
- [24] H. Ebert, D. Ködderitzsch, J. Minár, *Rep. Progr. Phys.* 74 (2011) 096501.
- [25] P. Lloyd, P.V. Smith, *Adv. Phys.* 21 (1972) 69.
- [26] R. Zeller, *J. Phys.: Condens. Matter* 20 (2008) 035220.
- [27] P.G. van Engen, K.H.J. Buschow, M. Erman, *J. Magn. Magn. Mater.* 30 (1983) 374–382.
- [28] R.Y. Umetsu, K. Kobayashi, A. Fujita, K. Oikawa, R. Kainuma, K. Ishida, N. Endo, K. Fukamichi, A. Sakuma, *Phys. Rev. B* 72 (2005) 214412.
- [29] S. Wurmehl, G.H. Fecher, C. Felser, *Z. Naturforsch.* 61b (2006) 749–752.
- [30] J. Kübler, G.H. Fecher, C. Felser, *Phys. Rev. B* 76 (2007) 024414.
- [31] K.H.J. Buschow, P.G. van Engen, R. Jongebreur, *J. Magn. Magn. Mater.* 38 (1983) 1–22.
- [32] M. Born, *J. Chem. Phys.* 7 (1939) 591–603.
- [33] R. Hill, *Proc. Phys. Soc. A* 65 (1952) 349.
- [34] E. Şaşıoğlu, L.M. Sañdratskii, P. Bruno, *J. Phys.: Condens. Matter* 17 (2005) 995–1001.
- [35] A.I. Liechtenstein, M.I. Katsnelson, V.P. Antropov, V.A. Gubanov, *J. Magn. Magn. Mater.* 67 (1987) 65–74.
- [36] P.W. Anderson, *Solid State Phys.* 14 (1963) 99–214.
- [37] S. Ram, M.R. Chauhan, A. Kunal, V. Kanchana, *Phil. Mag. Lett.* 91 (2011) 545–553.
- [38] D.P. Rai, R.K. Thapa, *J. Supercond. Nov. Magn.* 26 (2013) 3507–3513.
- [39] Benny G. Johnson, Peter M.W. Gill, John A. Pople, *J. Chem. Phys.* 98 (1993) 5612.
- [40] H.C. Kandpal, G.H. Fecher, C. Felser, *J. Phys. D: Appl. Phys.* 40 (2007) 1507.
- [41] M.A. Zagrebina, V.V. Sokolovskiy, V.D. Buchelnikova, O.O. Pavlukhina, *Physica B* 519 (2017) 82–89.
- [42] Y.V. Kudryavtsev, V.N. Uvarov, V.A. Oksenenko, Y.P. Lee, J.B. Kim, Y.H. Hyun, K.W. Kim, J.Y. Rhee, J. Dubowik, *Phys. Rev. B* 77 (2008) 195104.
- [43] Y. Miura, K. Nagao, M. Shirai, *Phys. Rev. B* 69 (2004) 144413.
- [44] A. Barducci, M. Bonomi, M. Parrinello, *WIREs Comput. Mol. Sci.* 1 (2011) 826–843.
- [45] D. Koller, F. Tran, P. Blaha, *Phys. Rev. B* 85 (2012) 155109.
- [46] D.J. Singh, *Phys. Rev. B* 82 (2010) 205102.
- [47] L. Van Hove, *Phys. Rev. B* 89 (1952) 1189–1193.
- [48] Ya. M. Blanter, M.I. Kaganov, A.V. Pantsulaya, A.A. Varlamov, *Phys. Rep.* 245 (1994) 159–257.
- [49] Y.O. Kvashnin, W. Sun, I. Di Marco, O. Eriksson, *Phys. Rev. B* 92 (2015) 134422.
- [50] P.V.S. Reddy, V. Kanchana, G. Vaitheeswaran, A.V. Ruban, N.E. Christensen, *J. Phys.: Condens. Matter.* 29 (2017) 265801.
- [51] K. Seema, *Intermetallics* 110 (2019) 106478.
- [52] P. Malavi, J. Song, W. Bi, A. Regnat, L. Zhu, A. Bauer, A. Senyshyn, L. Yang, C. Pfeleiderer, J.S. Schilling, *Phys. Rev. B* 98 (2018) 054431.